Picosecond excite-and-probe absorption measurement of the $^4T_2$ state nonradiative lifetime in ruby

S. K. Gayen, W. B. Wang, V. Petričević, R. Dorsinville, and R. R. Alfano
Institute for Ultrafast Spectroscopy and Lasers, Physics Department, City College of New York, New York, New York 10031

(Received 21 May 1985; accepted for publication 17 June 1985)

In a picosecond excite-and-probe absorption measurement, a 527-nm picosecond pulse excites the $^4T_2$ state of the Cr^{3+} ion in ruby and a 3.4-μm picosecond probe pulse monitors the growth and decay of population in the ^2E state as a function of pump-probe delay. From the growth of population in the metastable ^2E state, an upper limit of 7 ps for the nonradiative lifetime of the $^4T_2$ state is determined.

Ruby (Cr^{3+}:Al_2O_3), the first material that lased, is one of the most well characterized systems. However, the nonradiative relaxation rate of the excited states of Cr^{3+} ion in Al_2O_3 crystal has not yet been measured experimentally with any precision. It is well known that ruby is a three-level laser system. The broad $^4T_2$ band serves as the pump state which rapidly relaxes nonradiatively to the metastable, lasing ^2E level. The lasing action arises from the $^2E \rightarrow {}^4A_2$ transition. Because of the relatively strong vibronic coupling of the $^4T_2$ state with the breathing modes and Jahn–Teller modes in ruby,[1] the $^4T_2 \rightarrow {}^2E$ transition is extremely fast, which in turn may account for the lack of any precise relaxation time measurement. However, knowledge about nonradiative transitions is necessary to understand the laser action in solid state lasers. In this letter, we present a direct, time-resolved measurement of the $^4T_2$ nonradiative lifetime in ruby using the picosecond excite-and-probe spectroscopic technique.

The literature dealing with the relaxation times of the nonradiative transitions in ruby and transitions from the $^4T_2$ state in particular, covers a period of more than two decades. The theoretical and experimental estimates of the lifetime of the $^4T_2$ state in ruby also have a very wide range, from 10^{-6} to 10^{-13} s. While the theoretically predicted value is as low as 10^{-13} s, experiments have only provided upper limits to the lifetime, the lowest so far being 0.3 ns.[2–16] In the present work, we use a picosecond excite-and-probe arrangement to study transitions from the $^4T_2$ state in ruby. A 7-ps, 527-nm pump pulse excites the broad $^4T_2$ band. The excited $^4T_2$ state relaxes predominantly via nonradiative transitions resulting in a growth of population in the metastable ^2E state.[17] The growth of the population in the ^2E state is monitored by a 3.4-μm picosecond probe pulse. The terminal state of the probe transition is the $^4T_2$ band.

When the duration T of the pump pulse is much shorter than the relaxation times involved, so that it may be approximated by a δ function, the population in the ^2E state at time $t > T$ is given by

$$N(t) \approx N_0[1 - \exp(-t/\tau_1)]e^{-t/\tau_2}, \quad (1)$$

where N_0 is the population of $^4T_2$ state just after the excitation pulse, τ_1 and τ_2 are lifetimes of $^4T_2$ and ^2E states, respectively. Since τ_2 is of the order of milliseconds, for $\tau_1 \ll t \ll \tau_2$ Eq. (1) reduces to

$$N(t) \approx N_0[1 - \exp(-t/\tau_1)]. \quad (2)$$

In this case, $^4T_2$ lifetime may be obtained from a semilog plot of $N(t)$ versus time. If T is greater than or comparable to the relaxation time τ_1, then the growth of population in the ^2E state is governed by a convolution integral of the temporal profile of the pump pulse and the relaxation rate of the $^4T_2$ state. The time T may then only be considered as an upper limit for the lifetime.[11,12] In our measurement, the latter situation exists, and we obtain an upper limit for the $^4T_2$ lifetime.

A schematic diagram of the experimental arrangement

 0003-6951/85/170455-03$01.00

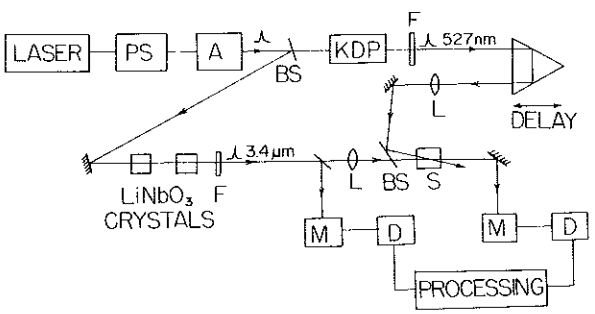

FIG. 1. Schematic diagram for the picosecond excite-and-IR-probe absorption apparatus. (Key: A = amplifier, BS = beamsplitter, D = infrared detector, F = filter, L = lens, M = monochromator, PS = single pulse selector, S = sample.)

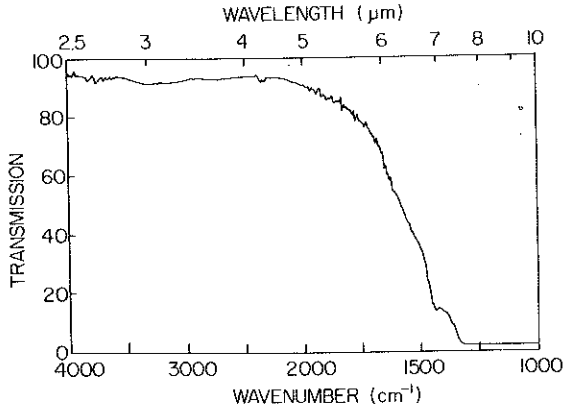

FIG. 2. Infrared transmission spectrum of ruby at room temperature.

for picosecond excite-and-infrared (IR) probe absorption measurements is shown in Fig. 1. A single 7-ps pulse is selected from a passively mode-locked Nd:glass laser and is amplified through three stages to about 50 mJ. A beamsplitter sends a fraction of this 1054-nm pulse through a phase-matched KDP crystal to generate 527 nm pump pulse. Another fraction goes through two $LiNbO_3$ crystals to generate the IR probe pulse which may be wavelength tuned from 2 to 5 μm by angle tuning the $LiNbO_3$ crystals. The time delay between the pump and the probe pulses may be varied by using an optical delay line. The pulse repetition rate for the laser is one in two minutes.

The ruby sample used in this experiment was obtained from Adolf–Meller Co. and had a 0.04% Cr_2O_3 by weight which is equivalent to a Cr^{3+} ion concentration of 1.3×10^{19} cm^{-3}. The sample was in the form of a cylinder 4.5 mm long and 9 mm in diameter, with its c axis parallel to the axis of the cylinder. The absorption measurements were taken through the 4.5-mm path length of the sample. Both the pump and the probe pulses were linearly polarized at right angles to the c axis of the ruby sample.

A ground-state infrared transmission spectrum of the ruby sample is shown in Fig. 2. This was taken to determine the window-wavelength range (in IR), where there is little ground-state absorption. From this measurement a wavelength of 3.4 μm was chosen for the probe pulse. The pump pulse was focused to a 0.8-mm-diam spot on the sample by a 25-cm focal length lens. Another 10-cm focal length lens focused the probe pulse on the sample to a 0.6-mm-diam spot. The two pulses traverse the sample almost collinearly (a crossing angle of 2°), and great care is taken to ensure good overlap between the two pulses. The transmitted probe pulse is passed through a monochromator. Its intensity I_s is measured by a liquid-nitrogen-cooled InSb photovoltaic detector at the exit slit of the monochromator. A beamsplitter directs a fraction of the probe pulse through an identical monochromator detector combination to monitor the intensity I_r of the probe pulse before the sample. Short term random fluctuations in the probe-pulse intensity are corrected for by taking the ratio (I_s/I_r) of the transmitted probe pulse intensity to the intensity of the reference probe pulse thus measured. To improve the signal-to-noise ratio, this normalized probe intensity was averaged over ten laser pulses.

For the excite-and-probe absorption measurements, first the pump pulse is blocked and the normalized probe intensity $(I_s/I_r)_u$ is measured. This fixes the baseline for induced absorption measurement. Then the pump pulse at 527 nm excites the sample. The 3.4-μm probe pulse samples the excited volume, and the normalized probe intensity $(I_s/I_r)_p$ is measured. The normalized intensity of the probe beam depends on the changes initiated in the sample by the exciting pulse. The change in optical density (OD) for a given pump-to-probe delay time is given by

$$\Delta\,\mathrm{OD}(t)=\log\left(\frac{(I_s/I_r)_u}{(I_s/I_r)_p}\right), \tag{3}$$

where the subscripts u and p stand for unpumped and pumped conditions of the sample. The kinetics of the excit-

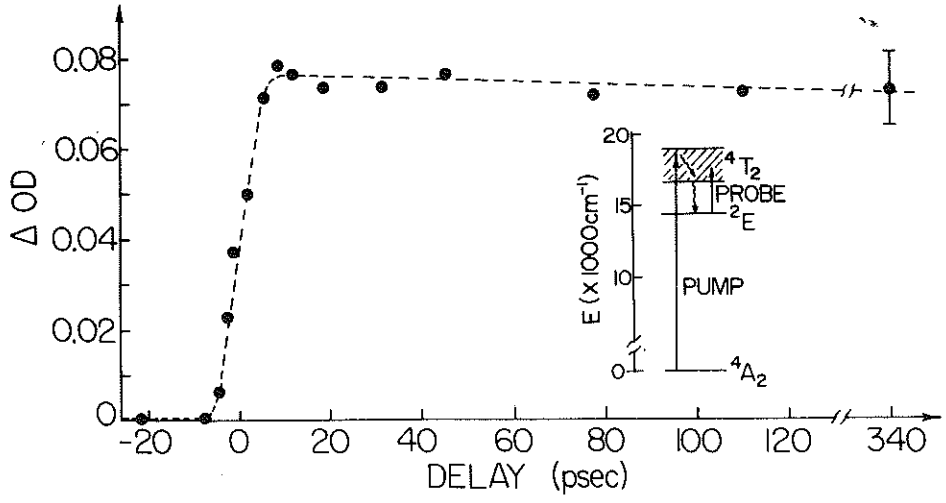

FIG. 3. Rise and decay of population in the excited ^2E state probed by a 3.4-μm pulse following excitation of the $^4T_2$ level in ruby by a 7-ps 527-nm pulse. Inset shows the relevant energy level diagram of Cr^{3+}:Al_2O_3, and the pump, probe, and relaxation transitions. The zero time is accurate within 5 ps. Size of a typical error bar is shown.

ed-state transitions is studied by measuring $\Delta\,\mathrm{OD}(t)$ as a function of pump-probe delay. Typically, a $\Delta\,\mathrm{OD}\approx 0.025$ may be measured using this apparatus. The change in optical density gives a direct measure of the population in the ^2E state.

The time evolution of optical density at 3.4 μm in the ^2E state at room temperature is displayed in Fig. 3. The salient features of the curve are a rapid rise followed by a long decay. The long lifetime decay reflects the depopulation of ^2E state, which shows no appreciable change over the time scale of this measurement. This is expected since the lifetime of the ^2E state at room temperature is 3 ms. The rise time for population in the ^2E state (time for growth of population from 10% to 90%) is ~ 10 ps. The rise time is limited by the duration of the pump pulse. This leads to an experimentally determined, shortest-so-far upper limit of ~ 7 ps for the $^4T_2$ lifetime in ruby. Measurements using a subpicosecond setup which produces 150-fs pulses with the visible supercontinuum are now in progress to determine more precisely the $^4T_2$ lifetime in ruby and other Cr^{3+}-doped crystals.

We would like to acknowledge Dr. J. Buchert and Dr. N. Ockman for their discussion and help, and NASA and ARO for financial support.

[1]R. Englman, B. Champagnon, E. Duval, and A. Monteil, J. Lumin. **28**, 337 (1983).
[2]T. H. Maiman, Phys. Rev. Lett. **4**, 564 (1960).
[3]A. Kiel, in *Quantum Electronics, Proceedings of Third International Congress*, edited by P. Grivet and N. Bloembergen (Columbia University, New York, 1963), Vol. 1, p. 765.
[4]B. Z. Malkin, Fiz. Tverd. Tela **4**, 2214 (1962) [Sov. Phys. Solid State **4**, 1620 (1963)].
[5]A. Misu, J. Phys. Soc. Jpn. **19**, 2260 (1964).
[6]P. Kisliuk and C. A. Moore, Phys. Rev. **160**, 307 (1967).
[7]J. Brossel and J. Margerie, in *Paramagnetic Resonance*, edited by W. Low (Academic, New York, 1963), Vol. II, p. 535.
[8]Joseph A. Calviello, Edward W. Fisher, and Zindel H. Heller, J. Appl. Phys. **37**, 3156 (1967).
[9]W. H. Fonger and C. W. Struck, Phys. Rev. B **11**, 3251 (1975).
[10]B. S. Tsukerblat and Yu. E. Perlin, Fiz. Tverd. Tela **7**, 3278 (1965) [Sov. Phys. Solid State **7**, 2647 (1966)].
[11]S. A. Pollack, IEEE J. Quantum Electron. **4**, 703 (1968).
[12]S. A. Pollack, J. Appl. Phys. **38**, 5083 (1967).
[13]M. Anson and R. C. Smith, IEEE J. Quantum Electron. **6**, 268 (1970).
[14]Patrick N. Everett, J. Appl. Phys. **42**, 2106 (1971).
[15]J. E. Rives and R. S. Meltzer, Phys. Rev. B **16**, 1808 (1977).
[16]M. Montagna, O. Pilla, and G. Viliani, Phys. Rev. Lett. **45**, 1008 (1980).
[17]The $^4T_2 \rightarrow {}^2E$ relaxation may proceed through the $^2T_1$ state, i.e., in the $^4T_2 \rightarrow {}^2T_1 \rightarrow {}^2E$ sequence. However, it has been pointed out[1] that this channel is not efficient for the transition. Also, $^2T_1$ state decays quickly to ^2E. So, in this work the population of $^2T_1$ is added to ^2E, the two levels together forming a metastable doublet. This assumption does not affect the $^4T_2$ lifetime since it is the depopulation rate of $^4T_2$ state that matters.

